JOURNAL OF SOLID STATE CHEMISTRY **100**, 136–140 (1992)

Magnetic Susceptibility and Electron Paramagnetic Resonance Studies of Tetravalent Terbium Ions in $BaTbO_3$ and $SrTbO_3$

YUKIO HINATSU

Department of Chemistry, Japan Atomic Energy Research Institute, Tokai-mura, Ibaraki 319-11, Japan

Received December 17, 1991; in revised form February 27, 1992; accepted March 3, 1992

Tetravalent terbium perovskites, $BaTbO_3$ and $SrTbO_3$, were prepared, and their magnetic susceptibilities and electron paramagnetic resonance (EPR) spectra were measured. Both the compounds showed antiferromagnetic transitions at 32.7 and 30.5 K, respectively. The effective magnetic moment of terbium is 7.96 μ_B, which is very close to the theoretical value of the Tb^{4+} ion. The EPR spectra could be measured at room temperature. The spectra were broad and the g-values of $BaTbO_3$ and $SrTbO_3$ were 2.00 and 1.97, respectively. These results also show that the oxidation state of terbium is not trivalent, but tetravalent. The deviation of the g-value from 2.00 for $SrTbO_3$ is due to the large crystal field distortion from octahedral symmetry around the terbium ion.

Introduction

The most stable oxidation state of rare-earth elements is trivalent. In addition to this state, cerium, praseodymium, and terbium have the tetravalent state (*1*). As a result, these elements form a series of oxide phases between M_2O_3 and MO_2 (M: rare earth). However, the preparative condition of terbium dioxide TbO_2 is very severe (*2*).

Mixed metal oxides ABO_3 with perovskite structure are known to incorporate various kinds of tetravalent metal ions at the B site of the crystals. Although many of the transition elements at the B site form perfect or nearly perfect cubic perovskite structures (*3*), the rare-earth ions are too large to stabilize the structure, and instead develop distorted perovskite structures. On the barium terbate $BaTbO_3$, Kemmler-Sack *et al.* reported that it crystallizes in an orthorhombically distorted perovskite structure and contains also trivalent terbium ions from the results of the optical and magnetic investigations (*4*). Jacobson *et al.* showed that $BaTbO_3$ is rhombohedrally distorted from the powder neutron diffraction (*5*) and found the antiferromagnetic ordering below 37 K (*6*). On the contrary, Yoshimura *et al.* reported that the lattice symmetry of this $BaTbO_3$ is orthorhombic P_{bnm} (*7*).

In this study, we prepared two tetravalent terbium perovskites, $BaTbO_3$ and $SrTbO_3$. The samples were characterized by Cu$K\alpha$ X-ray diffraction. The magnetic susceptibilities and electron paramagnetic resonance (EPR) spectra were measured to elucidate the magnetic properties and the oxidation state of terbium in the compounds. In both compounds, magnetic exchange interactions were found. To clarify the nature of these interactions, solid solutions of

0022-4596/92 $5.00

$BaTbO_3$ and diamagnetic $BaCeO_3$ were prepared and their magnetic susceptibilities and EPR spectra were measured.

Experimental

1. Preparation

$BaTbO_3$. As the starting materials, $BaCO_3$ and Tb_4O_7 were used. The Tb_4O_7 was reduced to the stoichiometric Tb_2O_3 by heating in a flow of hydrogen gas at 1000°C for 8 hr. The $BaTbO_3$ was prepared by repeatedly grinding mixtures of $BaCO_3$ and Tb_2O_3 in the correct stoichiometric metal ratio and firing them in a flow of oxygen gas to 1300°C. Since the $BaTbO_3$ loses a few oxygens at high temperatures and is reoxidized to the stoichiometric composition during cooling (*8*), the sample was kept at 1000°C for 48 hr and cooled to room temperature in the furnace.

$SrTbO_3$. As the starting materials, $SrCO_3$ and Tb_2O_3 were used. Preparation procedures were the same as in the case of $BaTbO_3$.

$BaTb_{1-y}Ce_yO_3$. As the starting materials, $BaCO_3$, Tb_2O_3, and CeO_2 were used. Before use, CeO_2 was heated in air at 850°C to remove any moisture and oxidized to the stoichiometric composition. The $BaCO_3$, Tb_2O_3, and CeO_2 were weighed in the correct metal ratios (y = 0.05, 0.10, 0.15, ---, and 0.40), and well mixed. The heating procedures were the same as in the case of $BaTbO_3$. After cooling to room temperature, the samples were crushed into powder, re-pressed into pellets, and heated under the same conditions to make the reaction complete.

2. Analysis

An X-ray diffraction analysis was performed with Cu$K\alpha$ radiation on a Philips PW 1390 diffractometer equipped with a curved graphite monochromator. The lattice parameters of the samples were determined by a least-squares method. The oxygen concentrations of the samples were determined from the weight change during heating.

3. Magnetic Susceptibility Measurement

The magnetic susceptibility was measured by a Faraday-type torsion balance in the temperature range between 4.2 K and room temperature. The apparatus was calibrated with a Manganese Tutton's salt ($\chi_g = 10{,}980 \times 10^{-6}/(T + 0.7)$). The temperature of the sample was measured by a "normal" Ag vs Au–0.07 at%Fe thermocouple (4.2 ~ 40 K) (*9*) and Au–Co vs Cu thermocouple (10 K ~ room temperature). Details of the experimental procedure have been described elsewhere (*10*).

4. Electron Paramagnetic Resonance Measurement

The EPR measurements were carried out at room temperature using a JEOL 2XG spectrometer operating at 9.107 GHz with 100 kHz field modulation. The magnetic field was swept from 100 to 12,000 G. Before measuring the specimen, a blank was recorded to eliminate the possibility of interference by the background resonance of the cavity and/or sample tube. The magnetic field was monitored with a proton NMR gaussmeter, and the microwave frequency was measured with a frequency counter.

Results and Discussion

All of the reflections observed by X-ray powder diffraction for the $BaTbO_3$ were indexed using an orthorhombic cell and indicated a single phase. The lattice parameters refined by the least-squares method are listed in Table I. Although the crystal structure of $SrTbO_3$ was not determined, all the diffraction lines have been indexed in the orthorhombic system. The lattice parameters of $SrTbO_3$ are also listed in Table I.

TABLE I

LATTICE PARAMETERS OF $BaTbO_3$ AND $SrTbO_3$

Compounds	Parameters of the true cell (Å)	Parameters of the perovskite cell dimensions (Å)
$BaTbO_3$	$a' = 6.0440$	$a = c = 4.2799$
	$b' = 6.0615$	$b = 4.2709$
	$c' = 8.5417$	$\beta = 90.17°$
$SrTbO_3$	$a' = 5.8903$	$a = c = 4.1851$
	$b' = 5.9467$	$b = 4.1723$
	$c' = 8.3445$	$\beta = 90.55°$

Note. Accuracy ±0.001 Å and ±0.02°.

Details of both the crystal structures will be described elsewhere (*11*). From X-ray powder diffraction analysis, the orthorhombic solid solutions of $BaTbO_3$ and $BaCeO_3$ were found to be formed in a single phase. The compounds and solid solutions prepared in this study are listed in Table II. The results of the oxygen analysis indicate that in view of the error limits for this analysis, the specimens prepared in this study are considered to have entirely ideal perovskite stoichiometry and therefore we use the formula ABO_3 to describe our samples.

TABLE II

MAGNETIC PARAMETERS FOR $BaTb_{1-y}Ce_yO_3$ AND $SrTbO_3$

Compounds	μ_{eff} (μ_B)	θ (K)	T_N (K)
$BaTbO_{3.014}$	7.96	−54.8	32.7
$BaTb_{0.95}Ce_{0.05}O_{3.001}$	7.96	−52.9	30.6
$BaTb_{0.90}Ce_{0.10}O_{3.023}$	7.91	−51.3	28.0
$BaTb_{0.85}Ce_{0.15}O_{3.017}$	7.94	−47.7	26.0
$BaTb_{0.80}Ce_{0.20}O_{3.026}$	7.95	−45.1	—
$BaTb_{0.75}Ce_{0.25}O_{3.001}$	7.94	−43.5	—
$BaTb_{0.70}Ce_{0.30}O_{3.030}$	7.94	−38.2	—
$BaTb_{0.65}Ce_{0.35}O_{3.023}$	7.91	−35.5	—
$BaTb_{0.60}Ce_{0.40}O_{3.029}$	7.91	−33.3	—
$BaTb_{0.01}Ce_{0.99}O_{3.000}$	7.94	2.2	—
$SrTbO_{3.067}$	7.96	−52.5	30.5

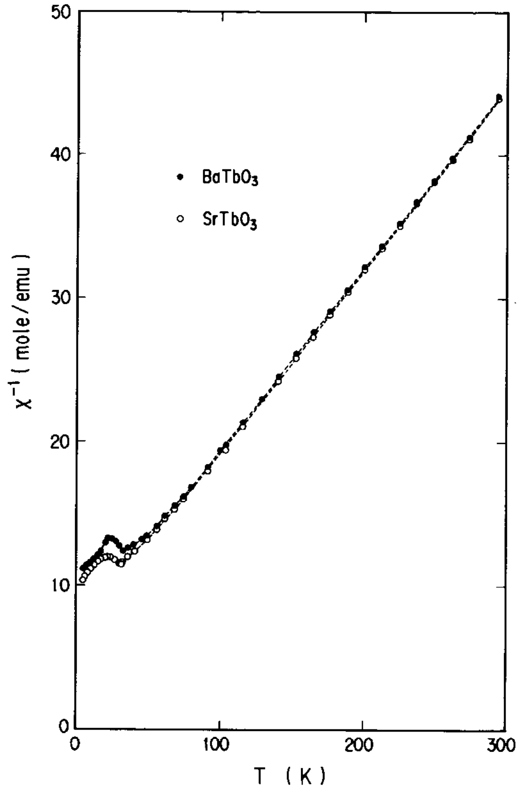

FIG. 1. Temperature dependence of reciprocal magnetic susceptibilities of $BaTbO_3$ and $SrTbO_3$.

Figure 1 shows the temperature dependence of reciprocal magnetic susceptibility for $BaTbO_3$. At 32.7 K, an antiferromagnetic transition was found. Tofield *et al.* (*6*) also reported the similar transition at 37 K, although neither the magnetic transition behavior nor the transition temperature were clear in their reciprocal magnetic susceptibility vs temperature curve. As shown in Fig. 1, the antiferromagnetic transition measured in this study is very clear. The temperature dependence of the susceptibility above 60 K follows the Curie–Weiss law with the Weiss constant $\theta = -54.8$ K. The effective magnetic moment of Tb^{4+} ion is 7.96 μ_B, which is very close to the theoretical effective magnetic moment (7.94 μ_B) for the $4f^7$ ion under the Russel–Saunders' cou-

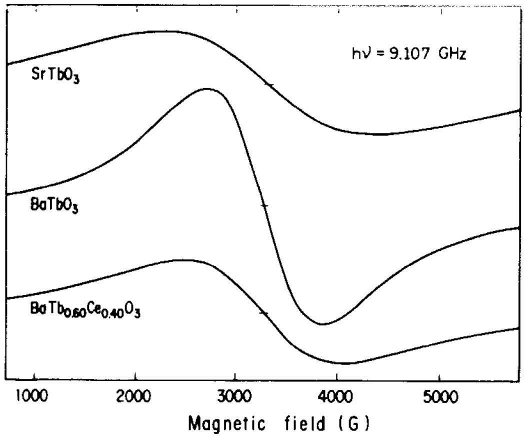

FIG. 2. EPR spectra of $BaTbO_3$, $SrTbO_3$, and $BaTb_{0.60}Ce_{0.40}O_3$.

pling scheme. This result indicates that the oxidation state of terbium is +4. If the oxidation state of terbium were +3 (the electronic structure of which is $[Xe]4f^8$), the effective magnetic moment should be 9.72 μ_B. The large Weiss constant (θ) shows the existence of magnetic exchange interactions at lower temperatures. When the Tb^{4+} ions are replaced by diamagnetic Ce^{4+} ions and diluted completely, the Weiss constant should approach zero and the effective magnetic moment should be 7.94 μ_B. The experimental results on the magnetic susceptibility of $BaTb_{0.01}Ce_{0.99}O_3$ (the Weiss constant of which is 2.2 K and the moment of Tb^{4+} is 7.94 μ_B) accord with this expectation. The temperature dependence of reciprocal magnetic susceptibility for $SrTbO_3$ is shown in Fig. 1. $SrTbO_3$ also shows the antiferromagnetic transition at 30.5 K. Above 60 K, the susceptibility follows the Curie–Weiss law ($\mu_{eff} = 7.96\ \mu_B$, $\theta = -52.5$ K).

It is well known that the EPR spectra for rare-earth ions can be measured only at very low temperatures because of the rapid spin–lattice relaxation (*12*). However, the situation is different for the rare-earth ions with half-filled *f* shell such as Gd^{3+}, Eu^{2+}, or Tb^{4+} because the ground states of them are *S*-states. So, if the oxidation state of terbium is tetravalent (the electronic configuration is $[Xe]4f^7$), the EPR spectrum should be observed. Figure 2 shows the EPR spectrum measured at room temperature. The observation of this spectrum strongly indicates that the oxidation state of terbium is not trivalent but tetravalent, because it is usually impossible to observe an EPR spectrum for a non-Kramers ion such as Tb^{3+} ($4f^{8+}$). The spectrum is very broad and the linewidth is 1160 G. The *g*-value is 2.00, which also supports, that the oxidation of terbium is tetravalent, because the ions with $4f^7$ configuration give the *g*-value (very near to) 2.00 (*12*). The EPR spectrum for $SrTbO_3$ is also depicted in Fig. 2. The EPR spectrum

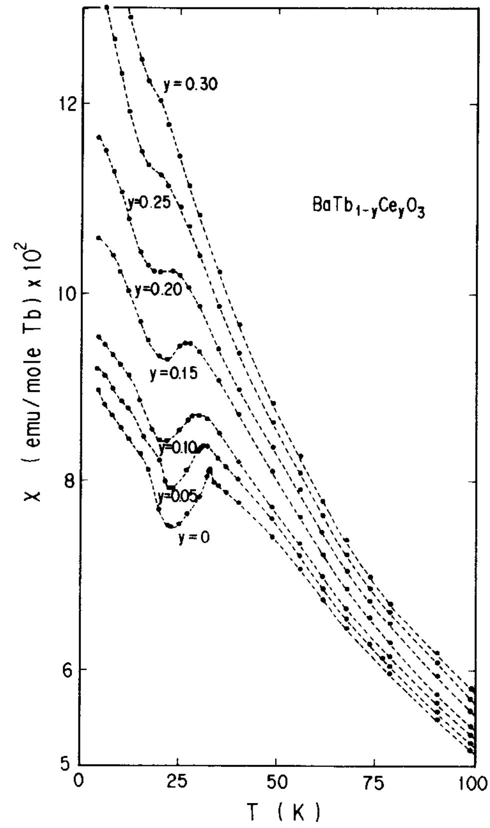

FIG. 3. Magnetic susceptibilities of $BaTb_{1-y}Ce_yO_3$ ($y = 0 \sim 0.30$) at low temperatures.

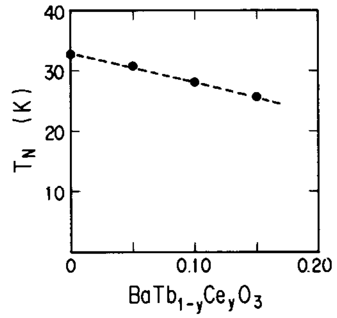

FIG. 4. Variation of T_N with cerium concentration, y.

becomes broader and the g-value departs from 2.00 and is 1.97, which is the result of the crystal-field effect on the magnetic properties. The crystal structures of $BaTbO_3$ and $SrTbO_3$ are orthorhombic. In the true crystallographic cell, there are four distorted perovskite pseudo-cells (*13*). They are monoclinic and their cell parameters are given in the right column of Table I. For $SrTbO_3$, the distortion from ideal perovskite structure (β value) is larger, i.e., the crystal-field distortion from octahedral symmetry around terbium ion is greater, which resulted in the deviation of g-value from 2.00.

To clarify the nature of magnetic interactions between terbium ions, solid solutions of $BaTbO_3$ diluted with diamagnetic $BaCeO_3$ were prepared and their magnetic susceptibilities and EPR spectra were measured. The susceptibility data are listed in Table II. Figure 3 shows the temperature dependence of magnetic susceptibility at low temperatures. As expected, the magnetic interactions between terbium ions were weakened and the Néel temperatures were lowered. For $BaTb_{0.80}Ce_{0.20}O_3$ solid solution, the antiferromagnetic transition was no longer found. In the range of this experiment, the Néel temperatures (T_N) decreased linearly with decreasing terbium concentration (Fig. 4), which is in accordance with the theory of magnetic dilution, but the critical concentration at which the antiferromagnetic disappears was not determined. With increasing cerium concentration, the EPR spectra were weakened and more broadened. As an example, the EPR spectrum of $BaTb_{0.60}Ce_{0.40}O_3$ is shown in Fig. 2. The line width is 1500 G, but the g-value remains $g = 2.00$.

References

1. N. E. TOPP, "Chemistry of the Rare-Earth Elements," Elsevier Amsterdam (1965).
2. J. B. MACCHESNEY, H. J. WILLIAMS, R. C. SHERWOOD, AND J. F. POTTER, *J. Chem. Phys.* **44**, 596 (1966).
3. R. W. G. WYCKOFF, "Crystal Structures (II)," Interscience, New York (1964).
4. S. KEMMLER-SACK AND I. HOFELISH, *Z. Naturforsch. B: Anorg. Chem. Org. Chem.* **26**, 539 (1971).
5. A. J. JACOBSON, B. C. TOFIELD, AND B. E. F. FENDER, *Acta Crystallogr., Sect. B* **28**, 956 (1972).
6. B. C. TOFIELD, A. J. JACOBSON, AND B. E. F. FENDER, *J. Phys. C* **5**, 2887 (1972).
7. M. YOSHIMURA, T. NAKAMURA, AND T. SATA, *Chem. Lett.* (9) 923 (1973).
8. M. YOSHIMURA, T. NAKAMURA, AND T. SATA, *Bull. Tokyo Inst. Technol.* (120) 13 (1974).
9. L. L. SPARKS AND R. L. POWELL, *J. Res. Nat. Bur. Stand. (U.S.)* **A76**, 263 (1972).
10. Y. HINATSU AND T. FUJINO, *J. Solid State Chem.* **60**, 195 (1985).
11. Y. HINATSU AND T. FUJINO, in preparation.
12. A. ABRAGAM AND B. BLEANEY, "Electron Paramagnetic Resonance of Transition Ions," Oxford Univ. Press, London (1970).
13. S. GELLER AND E. A. WOOD, *Acta Crystallogr.* **9**, 563 (1956).